



Published in final edited form as:

Biotechnol J. 2013 January ; 8(1): 117–126. doi:10.1002/biot.201200174.

Nanoscale Structure of Type I Collagen Fibrils: Quantitative Measurement of D-spacing

Blake Erickson^{1,2,#}, Ming Fang^{2,3,#}, Joseph M. Wallace⁷, Bradford G. Orr^{2,4,5}, Clifford M. Les⁶, and Mark M. Banaszak Holl^{1,2,3,4,*}

¹The University of Michigan Program in Biophysics, Ann Arbor, MI 48109

²Michigan Nanotechnology Institute for Medicine and Biological Sciences, Ann Arbor, MI 48109

³Department of Chemistry, Ann Arbor, MI 48109

⁴Program in Applied Physics, Ann Arbor, MI 48109

⁵Department of Physics, Ann Arbor, MI 48109

⁶Bone and Joint Center, Henry Ford Hospital, Detroit, MI 48202

⁷Biomedical Engineering, Indiana University-Purdue University, Indianapolis, 723 West Michigan Street, SL 220 Indianapolis, IN 46202-5132

Abstract

This paper details a quantitative method to measure the D-periodic spacing of Type I collagen fibrils using Atomic Force Microscopy coupled with analysis using a 2D Fast Fourier Transform approach. Instrument calibration, data sampling and data analysis are all discussed and comparisons of the data to the complementary methods of electron microscopy and X-ray scattering are made. Examples of the application of this new approach to the analysis of Type I collagen morphology in disease models of estrogen depletion and *Osteogenesis Imperfecta* are provided. We demonstrate that it is the D-spacing distribution, not the D-spacing mean, that showed statistically significant differences in estrogen depletion associated with early stage *Osteoporosis* and *Osteogenesis Imperfecta*. The ability to quantitatively characterize nanoscale morphological features of Type I collagen fibrils will provide important structural information regarding Type I collagen in many research areas, including tissue aging and disease, tissue engineering, and gene knock out studies. Furthermore, we also envision potential clinical applications including evaluation of tissue collagen integrity under the impact of diseases or drug treatments.

Keywords

Collagen fibril; D-spacing; 2D FFT; AFM

Additional correspondence: Prof. Joseph M. Wallace Department of Biomedical Engineering 723 W. Michigan SL220D Indiana University - Purdue University Indianapolis Indianapolis, IN 46202 jmwalla@iupui.edu Prof. Bradford G. Orr Department of Physics 450 Church Street University of Michigan Ann Arbor, MI 48109 orr@umich.edu. ***Correspondence:** Department of Chemistry University of Michigan 930 N. University Ave. Ann Arbor, MI 48109-1055 Telephone: (734) 763-2283 Fax: (734) 763-2283 mbanasza@umich.edu ;

#These authors contributed equally to this manuscript.

CONFLICT OF INTEREST: The authors declare no commercial or financial conflict of interest.

INTRODUCTION

Collagens are the most abundant family of structural proteins in animals [1, 2]. These proteins are based on trimeric polypeptide chains, each of which includes a repeating Gly-X-Y triplet region where X and Y are often proline and hydroxyproline. A major class of collagen is the fibrillar-forming type (type I, II, III, V, and XI), which has an approximately 300 nm long, uninterrupted triple helix[3]. Type I collagen accounts for 70% of all collagens and it is found throughout the body in the extracellular matrices (ECMs) of teeth, bones, tendons, skin, arterial walls and cornea[4].

At the nanoscale, the most prominent feature of Type I collagen fibrils is the ~67 nm axial D-periodic spacing. This feature was observed by X-ray diffraction[5] and imaged by transmission electron microscopy (TEM) as early as 1942 by Schmitt et al[6]. In 1963, the first model of the fibrillar structure was developed by Hodge and Petruska[7]. They proposed that molecules within a fibril are arranged in a staggered parallel alignment, resulting in “gap” and “overlap” regions[7]. Since this original description, X-ray diffraction[8-11] and electron microscopy[12-14] studies have supported a singular spacing of 67 nm. More detailed models of fibrillar structure have been elucidated by the effort of many researchers, including Miller, Brodsky, Hulmes, and Orgel, to name a few [9, 15-22]. We now know that a fibril is composed of five-stranded microfibrils which are supertwisted in the axial direction[22] and quasi-hexagonally packed in the equatorial plane[16]. An atomistic-scale-up simulation based on the state-of-the-art fibril model has elegantly shown the bottom-up design of a collagen fibril resulting in the D-periodicity[23]. Yet all such models are built upon this single valued 67 nm periodicity. Despite this commonly held view of a singular spacing, the hierarchical complexity of the collagen fibril itself, the variety of tissues into which these fibrils are incorporated, and the potential for morphological variation with damage and disease suggests that a single spacing value for all fibrils is unlikely. Recently, a quantitative approach to measuring this feature allowed the discovery of a distribution of D-periodic spacings ranging from ~60-73 nm in normal bone, dentin, skin, and tendon tissue[24]. This distribution changes as a function of estrogen depletion[25, 26] and *Osteogenesis Imperfecta* (OI)[27]. This new approach to understanding nanoscale collagen morphology is applicable to understanding the structure of collagen in a wide variety of tissues and ECM-linked diseases.

Quantitative analysis of morphological features in Type I collagen-based tissues is imperative to the understanding of normal tissue architecture[24]. This understanding is requisite for interpretation of any alterations caused by damage and disease. These methods may also serve as techniques for disease diagnosis in collagen-based tissues[25-27]. In this paper, we provide important experimental methodology for the application of atomic force microscopy to the quantitative analysis of Type I collagen D-spacing values. This includes approaches to instrument calibration, data sampling and analysis, and the comparison of the D-spacing values obtained with this method to complementary approaches including electron microscopy[12] and X-ray scattering[28]. The experimental approaches should prove useful for quantifying the changes in collagen structure for a wide range of diseases related to the extracellular matrix.

MATERIALS AND METHODS

Animals

Five year-old Columbia-Rambouillet cross sheep were anesthetized and ovariectomized (OVX) or subjected to a sham surgery (Colorado State University, ACUC # 03-010A-02). After 2 years, the ewes were sacrificed with an intravenous overdose of a barbiturate, and skin samples from the dorsal thoracolumbar region were used as previously described[29].

Atomic Force Microscopy (AFM) calibration

Calibration of the Agilent 5500 AFM large scanner (80 μm scan range) was carried out with a 100 nm x 100 nm calibration standard (NANOSENSORS, Switzerland), using contact mode and SNL-10 AFM probes (nominal tip radius 2 nm, force constant 0.25 N/m. Bruker AFM probes, CA). The scan size was set at 3.5 μm (35 \times 35 pitches) with 512 \times 512 pixels and a scan rate of 2 lines/sec. The absolute error of the calibration standard was verified by Scanning Electron Microscopy (SEM) imaging to be less than 1.1 % (FEI NOVA SEM, FEI Company, OR; Supporting Figure S1). After calibration, the percentage errors of the AFM in the fast and slow scan direction were 0.98 % and 0.20 % respectively.

Atomic Force Microscopy imaging and analysis

Tissue samples were processed and imaged in air using a PicoPlus 5500 Atomic Force Microscope (AFM, Agilent) in tapping mode as previously described[24, 25, 27]. Water and air comparison was carried out using a Dimension Icon AFM (Bruker AXS, Santa Barbara, CA) in scansyst fluid and air imaging modes. Scansyst fluid+ AFM probes (Bruker probes, nominal tip radius 2 nm, force constant 0.7 N/m) was used in both water and air imaging, in order to reduce differences caused by different tip convolutions. Skin samples were imaged in DI water and then dried by wicking away the water followed by exposure to a gentle stream of air for 30 minutes before re-imaging the same region in air. Following image capture, a rectangular region of interest (ROI) was chosen along straight segments of individual fibrils (Figure 1A). The selected regions spanned consistent topographical features (i.e. from gap region to gap region and through the middle of a given fibril). For each evaluated fibril, a two dimensional Fast Fourier Transform (2D FFT) was performed in SPIP and the 2D power spectrum was analyzed to determine the value of the D-periodic spacing for that fibril.

Computation

Model collagen fibrils were constructed in Matlab (The Mathworks: Natick, MA) as a summation of translated Gaussians. The power spectra of these model fibrils were computed and analyzed to determine the D-periodic spacing (the peak of the power spectrum) and D-periodic uncertainty (the standard deviation of the distribution of D-periodic spacing observed in the power spectrum). The results were further analyzed and compared to results obtained from SPIP on real fibrils experimentally imaged using AFM.

Statistical Analyses

To investigate differences in fibril morphology due to estrogen deficiency, D-periodic spacing values measured from an individual sample were averaged, yielding a single mean value for that sample, and then statistically compared using One Way ANOVA. Histograms were computed using a 1.0 nm bin size. To examine differences in the distribution of fibril morphologies between sham and OVX sheep, the Cumulative Distribution Function (CDF) of each group was computed. The CDF shows what fraction of a given sample is contained up to a particular value, easily demonstrating differences between distributions in both mean and standard deviation. To test for statistical significance between distributions, two-sample Kolmogorov-Smirnov (K-S) tests were then applied to the data sets.

RESULTS AND DISCUSSION

Aspects of measuring the D-periodic Spacing in Type I Collagen Fibrils

The axial D-periodic spacing was chosen as the key metric of collagen fibril morphology in this study. This measure captures aspects of collagen's fibrillar structure that may be related to the state of the individual molecular triple helices, post-translational modifications and/or

cross-linking within the fibril. Although the functional mechanisms of these activities has not been elucidated, in many cases it has been shown that genetic modification, non-enzymatic cross-linking and other changes at the molecular level lead to significantly compromised bulk tissue properties[1]. As seen in Figure 1A, D-periodic spacing is well resolved by AFM, providing a potential biomarker linked to the state of collagen. Previous studies have relied primarily on line scans and 1D FFTs and did not perform quantitative analyses of larger data sets[30-33]. Line scans and 1D FFTs suffer from 2 major limitations. First, lateral resolution is limited by a combination of factors including the pixel size of the image (~ 7 nm in images from the current study) and the radius of curvature of the probe (< 10 nm). The periodic nature of the fibril can be exploited with a 1D-FFT to resolve the average spacing below the single pixel limit, similar to the optical concept of super-resolution[34]. By fitting the FFT in reciprocal space to a continuous function, resolution can be achieved that is better than the limits set by pixel-related binning or apparent limits set by the radius of the probe. This interpolation scheme allows selection of the peak maximum with accuracy to tenths of a nanometer. An example calculation of this error using experimental data is included in Supporting Discussion #1.

The second and more significant limitation of line scans and 1D FFTs is that they both rely on the user drawing a line along the length of a fibril, normal to the D-spacing[25]. From 1D FFT measurements on fibrils in the current study, as little as a 5° deviation away from normal can alter the value measured for the spacing by as much as 8% (a difference of 5.4 nm on a 67.0 nm measurement, Figure 2). Errors of this magnitude are larger than the population standard deviations noted below, masking important information within the distributions.

The type of error noted has provided a significant challenge to the observation of a distribution of D-period spacings in EM and AFM studies over the last seven decades. Employing a 2D FFT approach decouples the determination of the D-periodic spacing from user bias in line location and angle selection. An example image of a collagen fibril imaged by AFM and measured using a 2D FFT approach is shown in Figure 1. In order to minimize edge effects that can degrade resolution, a rectangular region of interest is drawn and extends from the edge of one gap zone to the edge of another gap zone, remaining within the width of the fibril. Figure 1B shows the 2D FFT power spectrum from the selected region. The red line passes through the maximum value in the fundamental peak, therefore corresponding to the D-periodic spacing along the normal direction of the gap/overlap axis. A 1D FFT along this line demonstrates that the D-periodic spacing, the second and third harmonics are visible and well resolved (Figure 1C).

The 2D FFT analysis can be used to interpret D-spacing data from electron microscopy (EM) and AFM images. We have chosen AFM owing to its ability in keeping the tissue specimens relatively close to their native condition during sample preparation and imaging [35]. Absolute dehydration is thought to disrupt collagen molecular structure and increase packing density within a fibril[36, 37]. The effect of absolute dehydration has been shown to reduce collagen D-spacing[38, 39]. This implies hydration differences in the collagen fibrils could influence the observed distribution of collagen D-spacing. In order to demonstrate the effect of surface air-drying on collagen fibril D-spacing, we compared the metrical parameters of dermal collagen fibrils imaged by AFM in water and air. Dermis tissue was selected for this analysis because of the high water content in its native environment. As shown in height images in Figures 3A and 3B, the fibril surface imaged in water has greater height variation than the air-dried surface. The height profiles illustrated by line scans (1) and (2) demonstrate an apparent swelling of the collagen fibrils, and possibly other matrix proteins such as proteoglycans, when imaged in water. Measurement of multiple fibrils indicated as much as a two- to four-fold increase in apparent fibril height in water relative to

air. Error images shown in Figures 3C and 3D demonstrate that fibril D-spacings can be directly observed in water and air, respectively. Using these images as well as 6 other sets, we were able to identify 20 fibrils with well-resolved D-spacing repeat units present in paired water and air images. Using 2D FFT analysis, the D-spacings from the 20 fibrils were analyzed and are presented in the air versus water scatter plot (Figure 3E). As illustrated in Figure 3E, there is no correlation in the small shifts in D-spacings observed as a function of water vs air imaging. Indeed, seven fibrils exhibited larger D-spacings in air and eleven exhibited larger D-spacings in water. Two fibrils were essentially unchanged. In addition to the direct comparison of individual fibril D-spacings, we also plotted the histogram and CDF including every fibril that was observed in either water (60 fibrils) or air imaging (73 fibrils) for the 7 paired air/water images (Figure 3F and 3G). The averages of fibril D-spacing in this analysis are 62.2 ± 2.0 nm and 63.1 ± 1.9 nm in water and air, respectively. The difference in absolute value of the average D-spacing for air vs water imaging obtained from Figures 3E and 3F of 0.9 nm is on the same order as our ability to measure the spacings using the 2D-FFT method (Supporting Figure S3). The impact of air-drying is small compared to the width of the D-spacing distribution as illustrated in Figure 1 (discussed in a later section). It is interesting to note that although the histogram and CDF (Figures 3F and 3G) indicate an average D-spacing increase of 0.9 nm upon air drying, the paired fibril data in Figure 3E indicates that this average is obtained by a mix of behaviors ranging from 0 to 4 nm changes in D-spacing and both increases and decreases in D-spacing. This is also reflected in the substantial red/blue overlap, indicated in purple, in the CDF plot (Figure 3G) and the p-value of 0.125 indicating a lack of statistical significance. In summary, within the reproducibility of the measurement, there is no difference in D-banding spacing between the samples measured in air vs water.

Analysis of D-periodic Spacing Measurements and Associated Uncertainties

The D-periodic spacing was modeled with a translated set of Gaussian functions, the amplitude and width of which were set by comparison to AFM images of Type I collagen fibrils (Figure 1A). The spacing between each gap was allowed to vary, and the sampling of the “numerical model fibril” was set to match experimental imaging conditions. The D-periodic spacing and its associated uncertainty were determined by fitting the FFT as shown in Supporting Figure S2. To put an upper bound on the uncertainty associated with measurements from experimental samples, this 2D FFT and fitting approach was also applied to collagen fibrils imaged in sheep bones (used as a control for a previously published experiment[25]). The D-periodic spacing was computed for fibrils from multiple locations within the bone using a maximum of 21 D-period repeat units (Supporting Table S1). The upper bound on the D-Period uncertainty, calculated as the mean of the standard deviations, was found to be 0.8 nm. This result sets the minimum bin size for histograms at 0.8 nm.

Sampling theory dictates that the uncertainty associated with the D-periodic spacing measurement should scale as the inverse of the number of repeat units, until the fundamental fibril variability is reached. The measured D-periodic spacing should also be independent of the sampling length scale (pixel size), provided the feature is well resolved. Supporting Figure S3 shows the results of varying both the sampling length along a model fibril, and the variability in D-periodic spacing within a fibril. To achieve a standard deviation of 0.8 nm or less, a minimum of 9 D-Period repeat units must be included in the 2D FFT analysis. This figure verifies that the 2D FFT method is insensitive to sampling length scales, given the $1/x$ dependence in both panels.

Making absolute x-y distance measurements with AFM and comparing absolute values measured in different studies has limitations. Absolute measurement relies on accurate calibration of AFM, which depends on the use of appropriate calibration standards,

consistent performance of the piezo-material and regular calibration test to maintain the consistency. Due to the nonlinear relationship between scan size and scanner error, calibration over the range of D-spacing measurement ($3.5 \mu\text{m} \times 3.5 \mu\text{m}$ in the current study) using a feature size comparable to the collagen D-spacing ($\sim 67 \text{ nm}$) is critical. We calibrated the AFM using a $100 \text{ nm} \times 100 \text{ nm}$ standard, and limited the scan error to 0.98 % and 0.20 % for X and Y direction at $3.5 \times 3.5 \mu\text{m}$ image size. For a fibril with 67 nm D-spacing, the absolute error in the AFM measurement is less than 1 nm. Note that AFM manufacturer recommended calibration procedure utilizes a $10 \mu\text{m} \times 10 \mu\text{m}$ calibration standard, which is 100 times larger than the collagen feature size. Non-linearities in the piezoelectric scanners introduce substantial error between these size scales as detailed in Supporting Discussion #2. Nevertheless, this calibration process only addresses the absolute calibration (accuracy) of the system. The calibration has no bearing on the differential sensitivity between measurements (precision), and does not limit one's ability to differentiate between population distributions measured using the same AFM with the same calibration parameters.

Thermal drift is another important issue to consider with any AFM imaging study. To investigate the impacts of thermal drift, a single $3.5 \mu\text{m} \times 3.5 \mu\text{m}$ location was scanned up and down continuously over 1.5 hours. Measurements of the same individual fibrils within each image were then made and compared. This situation is an exaggeration of the thermal drift that may occur during normal scanning and even in this case, the drift on the fibril D-spacing measurement was less than 2 nm (Supporting Figure S5). Over the time associated with taking 1-2 images for analysis at this size scale (less than 10 minutes), this drift is negligible. Regardless, to overcome this limitation and avoid problems that may originate from it, the vast majority of measured fibrils are selected to be within $\pm 45^\circ$ from the fast scan axis. We have analyzed this issue previously[24] and the data is reproduced here as Supporting Figure S6. Using data from normal bone samples, a data plot of D-periodic spacing as a function of the angle of the measured fibril was produced. If thermal drift in the slow scan direction was present in the data and leading to artifacts, bulges near -90 and 90 degrees (along the slow axis) would exist. As this was not the case, the effects of thermal drift are not considered a major contributing factor in these measurements.

When using a surface-based technique such as AFM, the slope of the surface is another factor to consider. Hard samples (bone and dentin) are polished in attempt to create a flat surface. However, to directly address sample slope, one can consider both experimental and theoretical approaches. In a previous study, collagen from the mouse tail tendon was directly adsorbed onto a mica surface[24]. Mica is often used a substrate because it is atomistically flat, meaning that observed topography is considered a characteristic of the sample and not the substrate. In this case, a distribution of spacings was still observed and the mean spacing value was not statistically different from either bone or dentin samples suggesting that slope in the bone and dentin samples was not responsible for the observed spacing distributions. Next, a theoretical surface is considered. Within a $30 \mu\text{m} \times 30 \mu\text{m}$ image, 500 nm of tilt would equate to 0.96° . A tilt of this magnitude, if projected directly onto the long axis of a fibril, would cause a 67 nm spacing value to become 66.99 nm. Any such minor difference would be dwarfed by the spread of sample values. Increasing this tilt to $5 \mu\text{m}$ (almost 10° of tilt) would change the projected value to 66.1 nm. To directly address this concern in AFM images of bone specimens from a previous study[25], unflattened topography images were analyzed. The largest tilt value observed in the $3.5 \mu\text{m} \times 3.5 \mu\text{m}$ images was 546 nm. Even in this situation with almost 9° of tilt, a spacing of 67 nm would become 66.2 nm. As demonstrated in previous publications using this technique [24, 25, 27, 29], this magnitude of tilt-induced difference cannot account for the large population shifts noted in cases of disease.

D-periodic Spacing Occurs with a Distribution of Values

This 2D FFT approach was applied to Type I collagen fibrils imaged within sham-operated sheep dermis using AFM (used as a control for a previously published experiment). The mean D-periodic spacing of the 624 measured fibrils was 62.3 nm, with a population standard deviation of 1.4 nm. Figure 1D shows these data plotted as a histogram with a bin size of 1.0 nm (based on the maximum observed variation along a single fibril of 0.8 nm shown above). Note that the mean D-spacing value in dermal collagen has been reported to be less than 67 nm[40]. This histogram demonstrates that normal bone contains fibrils with a distribution of D-periodic spacing values. A recent study demonstrated that this type of distribution also exists in other Type I collagen based tissues including dentin and tendon[24]. Based upon these studies, and other tissue samples measured to date[25, 27], the existence of a distribution of D-periodic spacings is a fundamental characteristic of Type I collagen. However, the currently accepted models of Type I collagen fibrillar structure completely overlook the presence of a distribution of spacing values[15]. For example, the possibility of a distribution was not discussed in a recent thorough book review of collagen structure and mechanics[1].

Previous studies have shown that D-spacing increases upon applying strain to a bone or tendon tissue[41-43]. Sasaki and coworkers have shown that tendon D-spacing changes by 3% (~ 2 nm) at 20 MPa of stress[41]; Puxkandl have shown a 1 nm change in tendon D-spacing at 3% macroscopic tissue strain[42]; Gupta and Zioupos reported 0.3 nm change in D-spacing at 1% tissue strain in bone[43]. In addition to D-spacing elongation, interfibrillar sliding and shearing of proteoglycan-rich matrix are also thought occur under conditions of tissue strain[42, 43]. The magnitude of D-spacing change as a function of applied strain is not large enough to explain the D-spacing distribution observed across multiple tissues, which has a typical range of 10 nm.

As a way to verify that this distribution is real and not caused by sample preparation or AFM imaging artifacts, the 2D FFT analysis was performed on previously published SEM images from human Achilles tendons (Figure 4, reproduced with permission[12]). Qualitatively, the fibrils in Figure 4A look similar to AFM images of collagen fibrils. Figure 4B shows the histogram results of the 2D FFT analysis from 13 observed fibrils within the image (the included scale bar was used to set the length scale). The mean D-periodic spacing was 66.9 nm with a population standard deviation of 1.6 nm. This mean value is well within the absolute experimental error of the AFM results. More importantly, a distribution of D-periodic spacings was observed in the SEM data.

To investigate a different non-surface-based method that has been used to analyze Type I collagen nanoscale morphology, previously published Small Angle X-Ray Scatter (SAXS) data from fresh, non-mineralized, turkey tendon samples were analyzed[28]. This analysis was performed to determine if the magnitude of distribution observed in D-period spacing is consistent with the observed peak widths from SAXS analyses of collagen. A modified Bertaut-Warren-Averbach (BWA) technique was used to determine what portion of the peak widths can be ascribed to the D-Period spacing (Figure 5)[44]. Full details of the analysis are provided as Supporting Discussion #3.

This analysis has two main findings. First, a D-Period spacing distribution is sufficient to explain the observed peak width in the X-Ray data. Second, the distribution width determined from the X-Ray analysis was comparable to the distribution width observed using the 2D-FFT technique on individual fibrils. One significant advantage of the AFM 2D-FFT technique is that the fundamental resolution limit is sufficiently small to directly observe the shape of the sample distribution. The modified BWA technique cannot generate

the sample distribution shape because the ability to fit the transformed data is insufficient to discriminate between different functional forms of an underlying distribution.

Statistical Comparison of D-periodic Spacing Distributions as a Function of Disease

The existence of a distribution of D-periodic spacings is an important observation, standing in contrast to the fixed 67 nm value put forth 49 years ago. Utilizing an OVX model in sheep which leads to estrogen depletion, an early model of osteoporosis, it was hypothesized that differences between normal skin and skin from animals with a known disease state could be detected through changes in collagen fibril morphology[26]. The mean D-periodic spacing of the Sham population was 62.3 nm, not significantly different than the 61.9 nm value in OVX samples ($p = 0.249$ using One Way ANOVA). When viewed as histograms (Figure 1D), there was an observable increase in the OVX population towards lower D-periodic spacing values. Observing qualitative population differences between the normal and diseased states was an important finding, but proving statistical significance was imperative. Population differences were further highlighted when viewing the data as Cumulative Distribution Functions (CDF, Figure 1E). The CDF plot from the Sham population was then compared to that of the OVX population using a Kolmogorov-Smirnov test (K-S test), chosen because it is a non-parametric comparison between distributions. This test is sensitive to changes in means as well as in the width of distributions, and does not require normally distributed data. The two-sample K-S test demonstrated a significant difference in the population distributions between Sham and OVX samples ($p < 0.001$). These methods were also applied to a mouse model of human type IV OI, where a known genetic mutation on collagen was created by substituting glycine with cysteine[27]. Similar to the estrogen depletion model, no significant difference was noted in the means of D-spacing between the brittle mouse bones and wild type bones. Significant differences were present in the population distributions of fibril spacings. We found 55% of brittle fibrils versus 75% of wild type fibrils within ± 1 standard deviation (66-70 nm) range, which contributed to the statistically different CDF plots [27].

The origin of a D-spacing distribution and mechanisms of D-spacing changes that operate in diseases such as osteoporosis and OI are still unclear. We are currently pursuing these questions in our lab. Estrogen plays important roles in regulating metabolism, cell activities[45], and collagen turn-over[46-48], *etc.* The change in D-spacing induced by estrogen depletion is a complex system to study. In the case of point mutation in OI, inserting a bulkier residue in the molecular structure disrupts or destabilizes the triple helical conformation, through molecular kinking[49], free energy changes[50], weakening of intermolecular adhesion and reduction of cross-links[51]. These effects may lead to a change in D-spacing.

Although the mechanisms leading to these changes found in estrogen deprived and OI tissues are still unclear, these studies provide evidence to show that collagen nanomorphology is altered, an important information that could potentially explain the compromised tissue properties, and be considered in disease diagnosis.

CONCLUDING REMARKS

This paper details a systematic method to measure and analyze nanoscale characteristics of Type I collagen fibrils using the D-periodic spacing as the key metric of nanoscale morphology. The ability to accurately measure the D-periodic spacing using a 2D-FFT approach led to the discovery of a distribution of Type I collagen morphologies in four tissue types, bone, dentin, dermis and tendon. The importance of these observations was highlighted by demonstrating that statistically significant changes in population distributions could be observed in disease models of estrogen depletion and *Osteogenesis Imperfecta*. The

facts that distributions were present in both normal and diseased fibril populations, and that there were significant changes in these distributions with multiple diseases, has important implications for the structural model of Type I collagen fibrils, and possibly to the diagnosis of Type I collagen-based diseases. This type of analysis shows promise for providing important structural information regarding Type I collagen in a wide variety of collagen-related ECM diseases and processes, such as photo aging, Ehlers-Danlos Syndrome, *Osteogenesis Imperfecta*, *Osteoporosis*, wound healing, tissue engineering, and gene knockout model systems. Future work will be focused on the broader application of this method in ECM disease diagnosis and mechanistic studies. This method may find clinical uses in disease diagnosis and is already being employed for assessment of drug therapeutics.

Supplementary Material

Refer to Web version on PubMed Central for supplementary material.

Acknowledgments

We thank Judy Poore and Jeff Harrison at the Microscopy & Image Analysis Laboratory, U of M, for technical services. This work was partially supported by the National Institute of Dental and Craniofacial Research (National Institutes of Health) through a Ruth L. Kirschstein National Service Award (Grant number 1F32DE018840-01 A1), the National Institutes of Arthritis and Musculoskeletal and Skin Diseases (Grant number AR50562), and a research grant from the Investigator Initiated Studies Program of Merck Sharp & Dohme Corp. The opinions expressed in this paper are those of the authors and do not necessarily represent those of Merck Sharp & Dohme Corp.

Abbreviations

ECM	extracellular matrix
OI	<i>Osteogenesis Imperfecta</i>
AFM	atomic force microscopy
SEM	scanning electron microscopy
CDF	Cumulative Distribution Function
K-S	Kolmogorov-Smirnov
BWA	Bertaut-Warren-Averbach

REFERENCES

- [1]. Fratzl, P., editor. Collagen: Structure and Mechanics. Springer; New York: 2008.
- [2]. Kadler KE, Holmes DF, Trotter JA, Chapman JA. Collagen fibril formation. *Biochemical Journal*. 1996; 316:1–11. [PubMed: 8645190]
- [3]. Kadler KE, Baldock C, Bella J, Boot-Hanford RP. Collagens at a glance. *J. Cell Sci*. 2007; 120:1955–1958. [PubMed: 17550969]
- [4]. Canty EG, Kadler KE. Procollagen trafficking, processing and fibrillogenesis. *J. Cell Sci*. 2005; 118:1341–1353. [PubMed: 15788652]
- [5]. Bear RS. Long x-ray diffraction spacing of collagen. *J. Am. Chem. Soc*. 1942; 64:727.
- [6]. Schmitt FO, Hall CE, Jakus MA. Electron microscope investigations of the structure of collagen. *J. Cell. Comp. Phys*. 1942; 20:11–33.
- [7]. Hodge, AJ.; Petruska, JA. Recent Studies with the Electron Microscope on Ordered Aggregates of the Tropocollagen Molecule. In: Ramachandran, GN., editor. *Aspects of Protein Structure*. Academic Press; New York: 1963. p. 289
- [8]. Bigi A, Koch MHJ, Panzavolta S, Roveri N, Rubini K. Structural aspects of the calcification process of lower vertebrate collagen. *Connect. Tissue Res*. 2000; 41:37–43. [PubMed: 10826707]

- [9]. Fraser RDB, MacRae TP, Miller A, Suzuki E. Molecular conformation and packing in collagen fibrils. *J. Mol. Biol.* 1983; 167:497–521. [PubMed: 6864807]
- [10]. Eikenberry EF, Brodsky B, Parry DAD. Collagen fibril morphology in developing chick metatarsal tendons: I. X-ray diffraction studies. *Int. J. Biol. Macromol.* 1982; 4:322–328.
- [11]. Brodsky, B.; Eikenberry, EF. Characterization of fibrous forms of collagen. In: Cunningham, Leon W.; F., DW., editors. *Methods Enzymol.* Academic Press; 1982. p. 127-174.
- [12]. Chapman JA, Tzaphlidou M, Meek KM, Kadler KE. The Collagen Fibril - a Model System for Studying the Staining and Fixation of a Protein. *Electron Microscopy Reviews.* 1990; 3:143–182. [PubMed: 1715773]
- [13]. Lin AC, Goh MC. Investigating the ultrastructure of fibrous long spacing collagen by parallel atomic force and transmission electron microscopy. *Proteins-Structure Function and Genetics.* 2002; 49:378–384.
- [14]. Arsenault AL. Image analysis of mineralized and non-mineralized type I collagen fibrils. *J. Electron Microsc. Tech.* 1991; 18:262–268. [PubMed: 1880599]
- [15]. Orgel J, Irving TC, Miller A, Wess TJ. Microfibrillar structure of type I collagen in situ. *Proc. Natl. Acad. Sci. U. S. A.* 2006; 103:9001–9005. [PubMed: 16751282]
- [16]. Hulmes DJS, Wess TJ, Prockop DJ, Fratzl P. Radial packing, order, and disorder in collagen fibrils. *Biophys. J.* 1995; 68:1661–1670. [PubMed: 7612808]
- [17]. Hulmes DJS, Miller A. Quasi-hexagonal molecular packing in collagen fibrils. *Nature.* 1979; 282:878–880. [PubMed: 514368]
- [18]. Fraser RDB, MacRae TP, Miller A. Molecular packing in type I collagen fibrils. *J. Mol. Biol.* 1987; 193:115–125. [PubMed: 3586015]
- [19]. Orgel JPRO, Miller A, Irving TC, Fischetti RF, et al. The in situ supermolecular structure of type I collagen. *Structure.* 2001; 9:1061–1069. [PubMed: 11709170]
- [20]. Trus BL, Piez KA. Compressed microfibril models of the native collagen fibril. *Nature.* 1980; 286:300–301. [PubMed: 7402317]
- [21]. Piez KA, Trus BL. A new model for packing of type-I collagen molecules in the native fibril. *Biosci. Rep.* 1981; 1:801–810. [PubMed: 7306686]
- [22]. Orgel JPRO, Irving TC, Miller A, Wess TJ. Microfibrillar structure of type I collagen in situ. *Proc. Natl. Acad. Sci. U. S. A.* 2006; 103:9001–9005. [PubMed: 16751282]
- [23]. Gautieri A, Vesentini S, Redaelli A, Buehler MJ. Hierarchical structure and nanomechanics of collagen microfibrils from the atomistic scale up. *Nano Lett.* 2011; 11:757–766. [PubMed: 21207932]
- [24]. Wallace JM, Chen Q, Fang M, Erickson B, et al. Type I Collagen Exists as a Distribution of Nanoscale Morphologies in Teeth, Bones, and Tendons. *Langmuir.* 2010; 26:7349–7354. [PubMed: 20121266]
- [25]. Wallace JM, Erickson B, Les CM, Orr BG, Banaszak Holl MM. Distribution of Type I Collagen Morphologies in Bone: Relation to Estrogen Depletion in Bone. *Bone.* 2010; 46:1349–1354. [PubMed: 19932773]
- [26]. Fang M, Liroff KG, Turner AS, Les CM, et al. Estrogen Depletion Results in Nanoscale Morphology Changes in Dermal Collagen. *J. Invest. Dermatol.* 2012; 132:1791–1797. [PubMed: 22437310]
- [27]. Wallace JM, Orr BG, Marini JC, Banaszak Holl MM. Nanoscale Morphology of Type I Collagen is Altered in the Brl Mouse Model of Osteogenesis Imperfecta. *J. Struct. Biology.* 2011; 173:146–152.
- [28]. Fratzl P, Fratlzelman N, Klaushofer K. Collagen Packing and Mineralization - an X-Ray-Scattering Investigation of Turkey Leg Tendon. *Biophys. J.* 1993; 64:260–266. [PubMed: 8431546]
- [29]. Fang M, Liroff GK, Turner AS, Les CM, et al. Estrogen Depletion Results in Nanoscale Morphology Changes in Dermal Collagen. *J. Invest. Dermatol.* 2012
- [30]. Habelitz S, Balooch M, Marshall SJ, Balooch G, Marshall GW. In situ atomic force microscopy of partially demineralized human dentin collagen fibrils. *Journal of Structural Biology.* 2002; 138:227–236. [PubMed: 12217661]

- [31]. Hassenkam T, Fantner GE, Cutroni JA, Weaver JC, et al. High-resolution AFM imaging of intact and fractured trabecular bone. *Bone*. 2004; 35:4–10. [PubMed: 15207735]
- [32]. Baranauskas V, Garavello-Freitas I, Jingguo Z, Cruz-Hofling MA. Observation of the bone matrix structure of intact and regenerative zones of tibias by atomic force microscopy. *Journal of Vacuum Science & Technology A*. 2001; 19:1042–1045.
- [33]. Kindt JH, Thurner PJ, Lauer ME, Bosma BL, et al. In situ observation of fluoride-ion-induced hydroxyapatite-collagen detachment on bone fracture surfaces by atomic force microscopy. *Nanotechnology*. 2007; 18
- [34]. Cremer C, Kaufman R, Gunkel M, Pres S, et al. Superresolution imaging of biological nanostructures by spectral precision distance microscopy. *Biotechnology Journal*. 2011; 6:1037–1051. [PubMed: 21910256]
- [35]. Wallace JM. Applications of atomic force microscopy for the assessment of nanoscale morphological and mechanical properties of bone. *Bone*. 2012; 50:420–427. [PubMed: 22142635]
- [36]. Buehler MJ, Keten S, Ackbarow T. Theoretical and computational hierarchical nanomechanics of protein materials: Deformation and fracture. *Progress in Materials Science*. 2008; 53:1101–1241.
- [37]. Mogilner IG, Ruderman G, Grigera JR. Collagen stability, hydration and native state. *J. Mol. Graphics Model*. 2002; 21:209–213.
- [38]. Price RI, Lees S, Kirschner DA. X-ray diffraction analysis of tendon collagen at ambient and cryogenic temperatures: Role of hydration. *Int. J. Biol. Macromol*. 1997; 20:23–33. [PubMed: 9110182]
- [39]. Habelitz S, Balooch M, Marshall SJ, Balooch G, Marshall GW Jr. In situ atomic force microscopy of partially demineralized human dentin collagen fibrils. *J. Struct. Biol*. 2002; 138:227–236. [PubMed: 12217661]
- [40]. Brodsky B, Eikenberry EF, Cassidy K. An unusual collagen periodicity in skin. *Biochimica et Biophysica Acta (BBA) - Protein Structure*. 1980; 621:162–166.
- [41]. Sasaki N, Shukunami N, Matsushima N, Izumi Y. Time-resolved X-ray diffraction from tendon collagen during creep using synchrotron radiation. *J. Biomech*. 1999; 32:285–292. [PubMed: 10093028]
- [42]. Puxkandl R, Zizak I, Paris O, Keckes J, et al. Viscoelastic properties of collagen: Synchrotron radiation investigations and structural model. *Philosophical Transactions of the Royal Society B: Biological Sciences*. 2002; 357:191–197.
- [43]. Gupta HS, Zioupos P. Fracture of bone tissue: The ‘hows’ and the ‘whys’. *Med. Eng. Phys*. 2008; 30:1209–1226. [PubMed: 18977164]
- [44]. Drits VA, Eberl DD, Srodon J. XRD measurement of mean thickness, thickness distribution and strain for illite and illite-smectite crystallites by the Bertaut-Warren-Averbach technique. *Clays and Clay Minerals*. 1998; 46:38–50.
- [45]. Haczynski J, Tarkowski R, Jarzabek K, Slomczynska M, et al. Human cultured skin fibroblasts express estrogen receptor alpha and beta. *Int. J. Mol. Med*. 2002; 10:149–153. [PubMed: 12119550]
- [46]. Dimitrios J,H, Ioannis I,A. Bone Remodeling. *Ann. N. Y. Acad. Sci*. 2006; 1092:385–396. [PubMed: 17308163]
- [47]. Brincaat MP, Baron YM, Galea R. Estrogens and the skin. *Climacteric*. 2005; 8:110–123. [PubMed: 16096167]
- [48]. Brincaat M, Moniz CJ, Studd JWW. Long-term effects of the menopause and sex hormones on skin thickness. *Br. J. Obstet. Gynaecol*. 1985; 92:256–259. [PubMed: 3978054]
- [49]. Chang S-W, Shefelbine Sandra J, Buehler Markus J. Structural and Mechanical Differences between Collagen Homo- and Heterotrimers: Relevance for the Molecular Origin of Brittle Bone Disease. *Biophys. J*. 2012; 102:640–648. [PubMed: 22325288]
- [50]. Lee KH, Kuczera K, Banaszak Holl MM. The severity of osteogenesis imperfecta: A comparison to the relative free energy differences of collagen model peptides. *Biopolymers*. 2011; 95:182–193. [PubMed: 20945334]

- [51]. Gautieri A, Uzel S, Vesentini S, Redaelli A, Buehler MJ. Molecular and mesoscale mechanisms of osteogenesis imperfecta disease in collagen fibrils. *Biophys. J.* 2009; 97:857–865. [PubMed: 19651044]

\$watermark-text

\$watermark-text

\$watermark-text

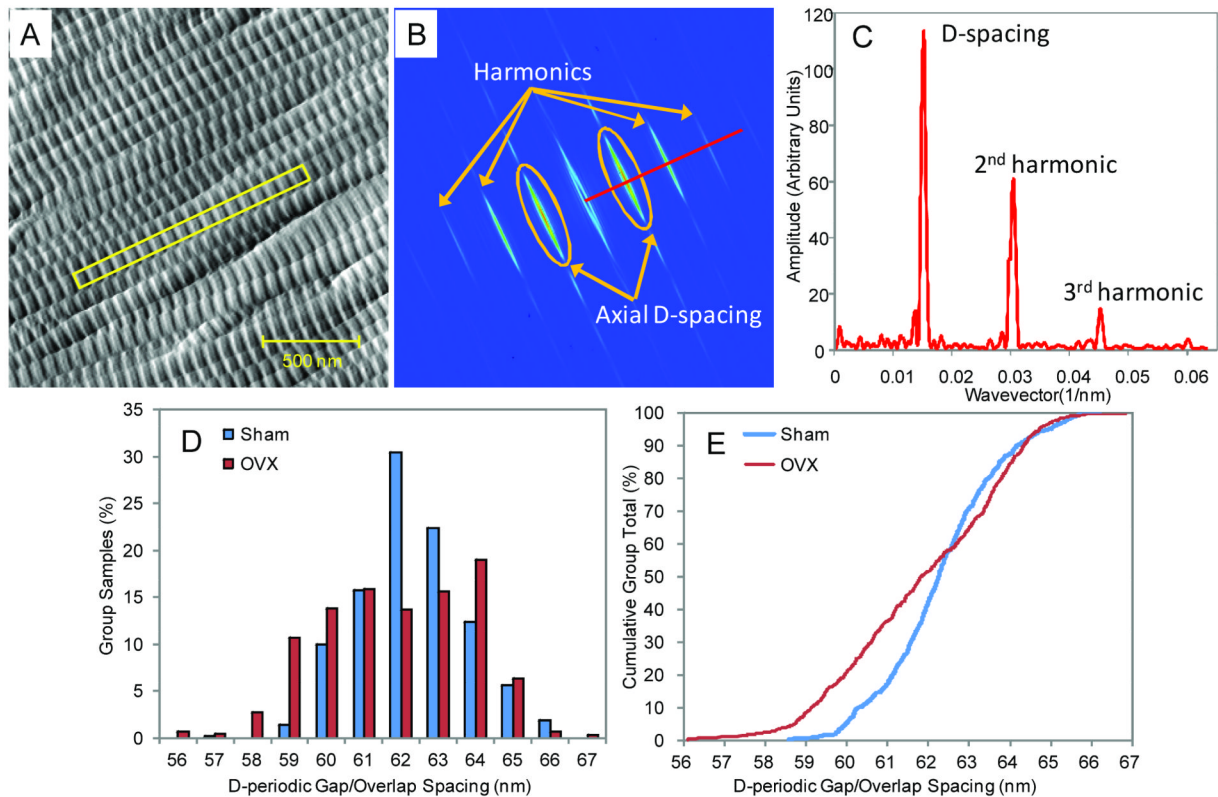


Figure 1. Schematic Representation of the 2D Fast Fourier Transform Process and D-periodic Spacing Measurements from Sham-Operated Versus Ovariectomized Sheep Dermis
 Panel A shows an AFM amplitude image of Type I collagen. The D-periodicity is visible as a striped pattern perpendicular to the fibril axis. Panel B shows the 2D FFT of the selected fibril. The red line runs through the maximum value of the first peak, corresponding to the D-periodic spacing. Panel C shows the 1D-FFT along this line, normal to the D-periodic spacing and through the maxima in the 2D power spectrum. Panel D and E are the histogram and Cumulative Density Functions (CDF) representation of Type I Collagen D-periodic spacing distributions analyzed by 2D FFT method. The comparison between Sham-operated versus estrogen-depleted (OVX) sheep dermis was derived from previously published work[26]. In this case, there was a significant increase of diseased populations towards lower D-periodic spacings.

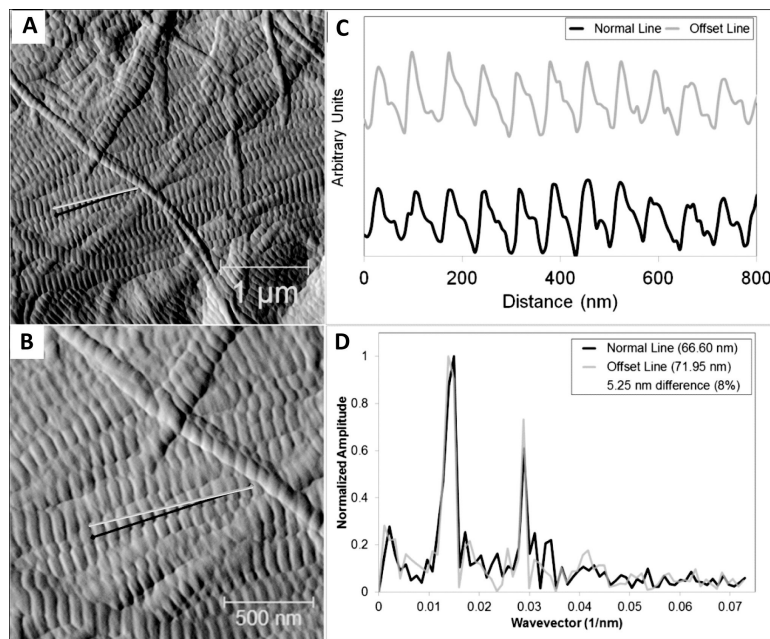


Figure 2. Effects of Angle on 1D FFT Measurements of D-Periodic Spacing

This figure demonstrates the effect of changing the angle of the user-drawn line on the D-periodic spacing measurement derived using a 1D FFT. Panel A is a $3.5 \mu\text{m} \times 3.5 \mu\text{m}$ amplitude image showing a fibril chosen for analysis. Panel B is an enlargement of the analyzed area. The same fibril was measured using a line drawn normal to the D-periodic spacing (black) and one with a 5° tilt from normal (blue line). Panel C shows the corresponding line scans from each line in panel B and panel D shows the 1D FFT derived from each line. In this example, there was a 5.4 nm difference in the measured D-periodic spacing (an 8% difference).

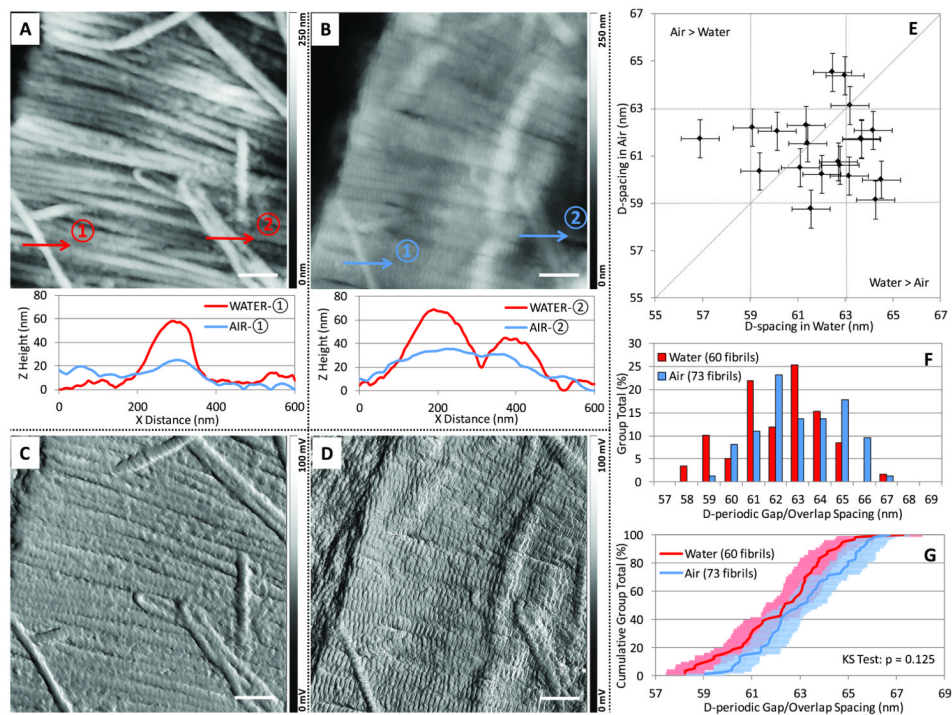


Figure 3. Comparison of Sheep Dermal Collagen D-spacings measured in water and air
 Panel A and B are height images of sheep dermal collagen fibrils imaged in water and air respectively (both panels A and B are baseline subtracted using 2nd order polynomial fitting). Selected height profiles in the fast scan direction were plotted for the comparison of fibril heights in water and air (the local minimum was set as 0 nm in height). Panel C and D are the error images for regions A and B, respectively. D-spacings from a set of 20 fibrils were measured both in water and air error images. The comparison is provided as a scatter plot (Panel E). Panels F and G are the histogram and CDF representation of the water versus air fibril D-spacings measurement for an uncorrelated set of 133 fibrils. In this case, all the fibrils with discernible D-spacing repeat units from a set of 7 images were included to generate the histogram in panel F and CDF in panel G. The error bars of 1.3 nm shown in Panels E and G were derived from a combination of the absolute measurement error and the uncertainty of the 2D-FFT fibril spacing assessment. The scale bar is 500 nm in panels A-D.

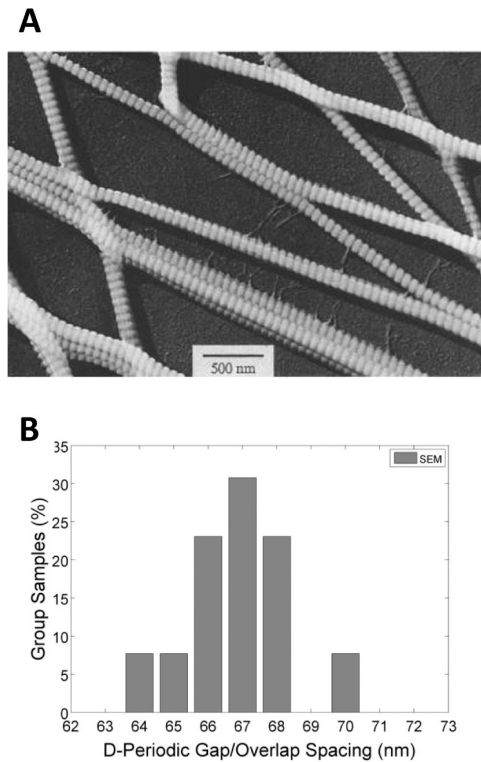


Figure 4. SEM Image of Type I Collagen Fibrils and Histogram of D-periodic Spacings
Panel A reproduces SEM images of isolated Type I collagen fibrils from Chapman et al. (reproduced with permission from Elsevier[12].) The D-periodic spacing of these fibrils was determined using the 2D FFT technique described above. The internal reference bar set the length scale. Panel B shows the distribution of D-periodic spacing values measured from 13 fibrils within the image. The distribution had a mean of 66.9 nm and a standard deviation of 1.6 nm. The presence of a distribution of spacings corroborates that the existence of a distribution is a real feature and not an imaging artifact.

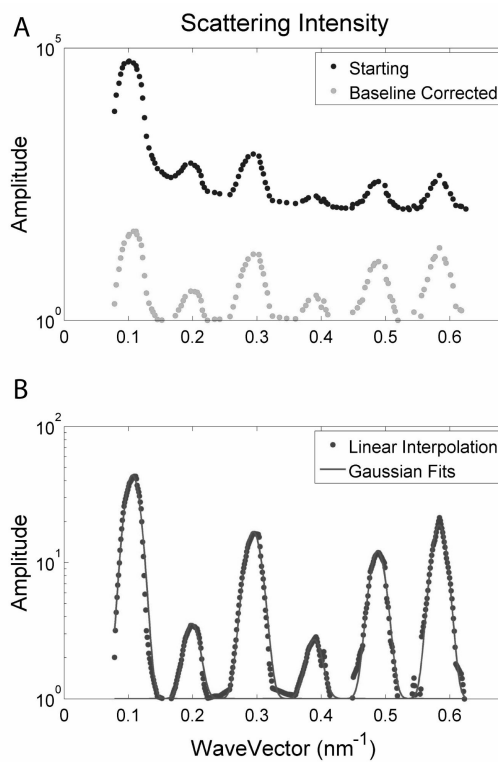


Figure 5. Analysis of SAXS Scattering Data from Fratzl et al.[28]

The extracted intensities are shown as blue dots. The red dots show baseline corrected data fit to the following background form: $Y = Ax^{-B} + C$ where $A = 1.1$, $B = -3.2$, $C = 10.9$. The green data is a linear interpolation of the red data so that all data points are equally spaced. Finally the teal lines are Gaussian fits to each scattering harmonic.